

# NATURAL PERIODS OF SEICHE IN LAKE SUWA AND LAKE NOJIRI AND ITS NUMERICAL MODEL

By

Goro Tomidokoro

Professor, Department of Architecture and Civil Engineering,  
Shinshu University, Nagano 380, Japan

and

Yasuhiro Akabori

Engineer, Nihonkensetu Consultant Co., Ltd., Tokyo, Japan

## SYNOPSIS

Natural periods of surface and internal seiche in Lake Suwa and Lake Nojiri are determined by using a numerical model on the one hand and from the field observation data of water temperature and free water level on the other. The finite element technique has been applied to describe the surface seiche behaviors and it has also been extended to the internal seiche.

The natural periods computed from the numerical model agree well with those obtained from observation data. The natural periods of first mode of the surface seiche in Lake Suwa and Lake Nojiri are about 1350s and 490s respectively, and those of the internal seiche in Lake Nojiri vary from 220 to 270 minutes.

## INTRODUCTION

Oscillation characteristics present in the natural periods of seiche in closed waters, lakes and ponds are very important to understand flow characteristics in closed waters. There are many studies concerning these problems in foreign countries but quite few in Japan. The oscillation periods, amplitudes and shapes were examined only in Lake Chuzenji (2), Lake Biwa (3), Lake Kasumi (4) and others.

In this paper, the natural periods of seiche in Lake Suwa and Lake Nojiri selected as typical shallow and deep lakes, respectively, are determined by means of a new numerical model and from the field observation data of free water level and water temperature in the thermocline region. So far, many numerical models of the natural periods of seiche in one-layered state have been introduced. In these models, an eigenvalue problem model(5) is proposed, which is obtained from two dimensional wave equations by using a finite element method. These wave equations are derived from the equations of continuity and motion, in which convective and viscous terms are neglected. This model can be applied to the lake with complicated lake shores and lake bottoms, but there is not such model, which can be applied to the two-layered lakes. Hence, in this paper, we extended above one-layered model and proposed a new model for prediction of the natural periods of seiche, that can be applied to the two-layered lakes with complicated lake shores and lake bottoms. And the validity of this model has been investigated by considering analytically solved examples and field observation results as well.

## NUMERICAL MODEL OF NATURAL PERIODS OF SEICHE

### Basic equations of seiche (1)

The  $x$  and  $y$  coordinates are taken on the undisturbed free surface and  $z$  coordinate vertically upward to  $x$ - $y$  plane, as shown in Fig.1. The densities of water in the upper and lower layers are assumed to be constant as  $\rho_1$  and  $\rho_2$ , respectively. Assuming that the horizontal length scale is very much larger than the water depth scale in the closed water, the hydrostatic assumption could be applied to the equations of motion of the  $z$  direction. Integrating over the upper and lower layers, respectively, the equations of motion of the  $z$  direction become

$$\left. \begin{aligned} p_1 &= \rho_1 g(\xi - z) \\ p_2 &= \rho_1 g(\xi + d) + \rho_2 g(-d - z) \end{aligned} \right\} \quad (1)$$

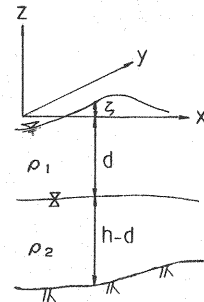


Fig.1 Definition sketch

in which  $p_1$  and  $p_2$  are the pressures for the upper and lower layers, respectively. We substitute Eq.(1) into the equations of motion of the  $x$  and  $y$  directions, in which convective and viscous terms are neglected because the flow is weak. By integrating them over the upper and lower layers, the following equations of motion are obtained.

$$\frac{\partial u_1}{\partial t} + g \frac{\partial \xi}{\partial x} = 0, \quad \frac{\partial v_1}{\partial t} + g \frac{\partial \xi}{\partial y} = 0 \quad (2)$$

$$\frac{\partial u_2}{\partial t} + g \left\{ \epsilon \frac{\partial (\xi + d')}{\partial x} - \frac{\partial d'}{\partial x} \right\} = 0, \quad \frac{\partial v_2}{\partial t} + g \left\{ \epsilon \frac{\partial (\xi + d')}{\partial y} - \frac{\partial d'}{\partial y} \right\} = 0 \quad (3)$$

in which  $(u_1, v_1)$  and  $(u_2, v_2)$  are the components of depth mean velocity for the upper and lower layers, respectively. It is also assumed that  $\epsilon = \rho_1/\rho_2$ ,  $d = \bar{d} + d'$  and  $\bar{d} \gg d'$  and  $\bar{d} \gg \xi$ . Furthermore, integrating the equations of continuity over the corresponding layer and using kinematic boundary conditions on the free and internal surfaces, we obtain

$$\frac{\partial (\xi + d')}{\partial t} + \bar{d} \left( \frac{\partial u_1}{\partial x} + \frac{\partial v_1}{\partial y} \right) = 0 \quad (4)$$

$$\frac{\partial (-d')}{\partial t} + (h - \bar{d}) \left( \frac{\partial u_2}{\partial x} + \frac{\partial v_2}{\partial y} \right) = 0 \quad (5)$$

Eliminating  $u_1$  and  $v_1$  from Eqs.(2) and (4), and  $u_2$  and  $v_2$  from Eqs.(3) and (5), respectively, we obtain

$$\frac{\partial^2 (\xi + d')}{\partial t^2} - g \bar{d} \left( \frac{\partial^2 \xi}{\partial x^2} + \frac{\partial^2 \xi}{\partial y^2} \right) = 0 \quad (6)$$

$$\frac{\partial^2 (-d')}{\partial t^2} - g (h - \bar{d}) \left\{ \epsilon \left( \frac{\partial^2 \xi}{\partial x^2} + \frac{\partial^2 \xi}{\partial y^2} \right) - (1 - \epsilon) \left( \frac{\partial^2 d'}{\partial x^2} + \frac{\partial^2 d'}{\partial y^2} \right) \right\} = 0 \quad (7)$$

Furthermore, adding Eq.(6) to Eq.(7), we obtain

$$\frac{\partial^2 \xi}{\partial t^2} - g \bar{d} \left( \frac{\partial^2 \xi}{\partial x^2} + \frac{\partial^2 \xi}{\partial y^2} \right) - g (h - \bar{d}) \left\{ \epsilon \left( \frac{\partial^2 \xi}{\partial x^2} + \frac{\partial^2 \xi}{\partial y^2} \right) - (1 - \epsilon) \left( \frac{\partial^2 d'}{\partial x^2} + \frac{\partial^2 d'}{\partial y^2} \right) \right\} = 0 \quad (8)$$

As a result, Eqs.(7) and (8) are the wave equations of seiche in the stratified closed water. Since the wave motion is harmonic, the following relationship

$$\zeta(x, y, t) = \beta(x, y) \cos(\sigma t), \quad d'(x, y, t) = \gamma(x, y) \cos(\sigma t) \quad (9)$$

can be assumed between  $(\zeta, d')$  and the maximum, or minimum, value  $(\beta, \gamma)$  at the particular coordinate location. Substituting Eq.(9) into Eqs.(7) and (8), we obtain

$$-\lambda^2 \beta - [(h - \bar{d})\epsilon + \bar{d}] \left( \frac{\partial^2 \beta}{\partial x^2} + \frac{\partial^2 \beta}{\partial y^2} \right) + (h - \bar{d})(1 - \epsilon) \left( \frac{\partial^2 \gamma}{\partial x^2} + \frac{\partial^2 \gamma}{\partial y^2} \right) = 0 \quad (10)$$

$$\lambda^2 \gamma - (h - \bar{d})\epsilon \left( \frac{\partial^2 \beta}{\partial x^2} + \frac{\partial^2 \beta}{\partial y^2} \right) + (h - \bar{d})(1 - \epsilon) \left( \frac{\partial^2 \gamma}{\partial x^2} + \frac{\partial^2 \gamma}{\partial y^2} \right) = 0 \quad (11)$$

where

$$\lambda^2 = \frac{\sigma^2}{g}, \quad \left( \sigma = \frac{2\pi}{T} \right) \quad (12)$$

where  $T$  is the period of oscillation.

Finite element discretization (5)

For the discretization of the basic equations, two variables are approximated as follows:

$$\beta = N_j \beta_j, \quad \gamma = N_j \gamma_j, \quad (j=i, j, k) \quad (13)$$

where  $N_j = N_j(x, y)$  is a shape function, and in this paper we use a standard linear function based on the three nodes  $(i, j, k)$  triangular finite element. Here and henceforth, the summation convention with repeated indices is employed. After substituting Eq.(13) into Eqs.(10) and (11), and integrating these equations which is multiplied by the weighting function  $N_i$  ( $j=i, j, k$ ) over the element, we obtain the following finite element equations for a single element.

$$\begin{aligned} \lambda^2 \left[ \int_S N_i N_i ds \right] \cdot \beta_i = & \left[ - \int_S [(h - \bar{d})\epsilon + \bar{d}] \left( \frac{\partial N_i}{\partial x} \frac{\partial N_j}{\partial x} + \frac{\partial N_i}{\partial y} \frac{\partial N_j}{\partial y} \right) \cdot ds \right] \cdot \beta_j \\ & + \left[ \int_S (h - \bar{d})(1 - \epsilon) \left( \frac{\partial N_i}{\partial x} \frac{\partial N_j}{\partial x} + \frac{\partial N_i}{\partial y} \frac{\partial N_j}{\partial y} \right) \cdot ds \right] \cdot \gamma_j, \end{aligned} \quad (14)$$

$$\begin{aligned} \lambda^2 \left[ \int_S N_i N_i ds \right] \cdot \gamma_i = & \left[ \int_S (h - \bar{d})\epsilon \left( \frac{\partial N_i}{\partial x} \frac{\partial N_j}{\partial x} + \frac{\partial N_i}{\partial y} \frac{\partial N_j}{\partial y} \right) \cdot ds \right] \cdot \beta_j \\ & - \left[ \int_S (h - \bar{d})(1 - \epsilon) \left( \frac{\partial N_i}{\partial x} \frac{\partial N_j}{\partial x} + \frac{\partial N_i}{\partial y} \frac{\partial N_j}{\partial y} \right) \cdot ds \right] \cdot \gamma_j, \end{aligned} \quad (15)$$

where we use the Green-Gauss theorem on the second order derivatives in Eqs.(10) and (11), and also the zero velocity conditions normal to the shore line. If there are many elements, the finite element equations are assembled for all elements by standard finite element procedure, and we obtain the global discretized equation in matrix form

$$\lambda^2 \begin{bmatrix} \mathbf{M}_{11} & \mathbf{0} \\ \mathbf{0} & \mathbf{M}_{22} \end{bmatrix} \begin{Bmatrix} \beta \\ \gamma \end{Bmatrix} = \begin{bmatrix} \mathbf{K}_{11} & \mathbf{K}_{12} \\ \mathbf{K}_{21} & \mathbf{K}_{22} \end{bmatrix} \begin{Bmatrix} \beta \\ \gamma \end{Bmatrix} \quad (16)$$

in which  $\mathbf{M}_{11}$ ,  $\mathbf{M}_{22}$ ,  $\mathbf{K}_{11}$ ,  $\mathbf{K}_{22}$ , etc. are the square matrices whose terms are the corresponding ones in the brackets multiplied by  $\beta_j$  and  $\gamma_j$  in Eqs.(14) and (15),  $\mathbf{0}$  the zero matrix,  $\beta$  and  $\gamma$  the column vectors whose terms are  $\beta_j$  and  $\gamma_j$ , respec-

tively. Therefore, Eq.(16) is reduced to an eigenvalue problem. Since the matrix of the right hand side of Eq.(16) is not symmetric, the equation is transformed into a asymmetric matrix. Then, the equation can be solved by means of standard computer programs.

#### Model application to analytically solved problems and Treatment of shallows

In order to examine the validity of above model, we compute the natural periods of seiche in a long rectangular lake, 100m in width, 5000m in length. The depths of bottom and internal surface are assumed to be constant, and are 20m and 10m, respectively, the specific density is  $\sigma = \rho_1/\rho_2 = 0.99/1.00$ . From the interfacial wave model(2) for the two-layered state, the analytical solutions for natural periods of internal seiche are 14286s, 7143s, etc, which are in good agreement with the numerical ones.

The natural periods of surface seiche can be obtained by this numerical model. So, by thinning the lower layer thickness and equaling its water density to that of upper layer, this model can be applied to the one-layered water. The values obtained by this numerical model according to above treatment agree well with the analytical ones,  $T = 2L/(gh)^{1/2} = 714s$ , etc., in which  $L$  is the lake length. The reason of the agreement is considered that Eq.(15) gives good approximation to the equation for the total water depth and the right hand side of Eq.(16) in this case is negligibly small, which gives extremely large natural periods.

From the above reason, the treatment of shallows, where the total water depths are smaller than the upper layer depths, is that we imagine a very thin lower layer near the bottom in shallows and the density of this layer is equal to that of upper layer, as shown in Fig.2.

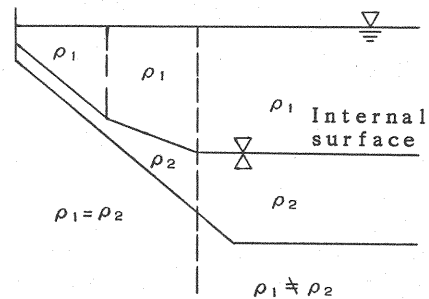


Fig.2 Treatment of shallows

#### OSCILLATION PERIODS OF LAKE SUWA AND LAKE NOJIRI

##### Lake Suwa and Lake Nojiri

Lake Suwa shown in Fig.3 is quite shallow and is 759m above the sea-level, 14.2km<sup>2</sup> in area, 18.3km in shore length, 6.8m in maximum depth and about 4.0m in mean depth. There is no shallows because all of the shores are protected by the embankments. A weak thermal stratification is formed after several fine and no wind days in summer but is easily mixed by weak winds. Thus, Lake Suwa is homogeneous during almost all the year. Lake Suwa is usually frozen over from the last ten days of January to February.

Lake Nojiri shown in Fig.4 has very complicated lake shores and lake bottoms and the deep water depth against to the lake area, those are peculiar to the mountain lake, and is 645m above the sea-level, 4.0km<sup>2</sup> in area, 14.0km in shore length, 42.0m in maximum depth, and about 18.7m in mean depth. The thermal stratification is formed from the beginning of summer to fall, and a typical two-layered state with a thin thermocline region is formed from September to the beginning of October. Lake Nojiri is frozen over from the last ten days of January to the first ten days of March.

##### Observation methods

To observe surface seiche behaviors, variances of the free Water level in the lake are measured by using a capacity type wave meter. In order to cut off the high frequency components of waves, the wave meter is installed in a vinyl chlo-

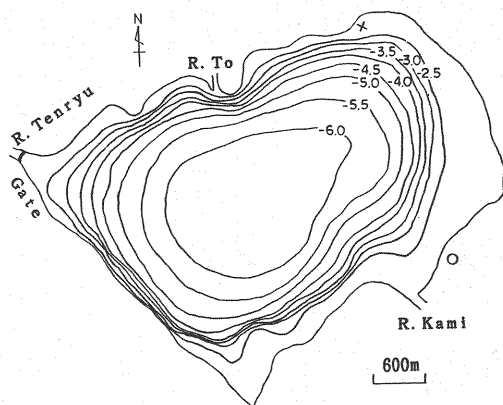


Fig.3 Topography of Lake Suwa  
(○ Suwa Meteorological station,  
× Observation station of water level)

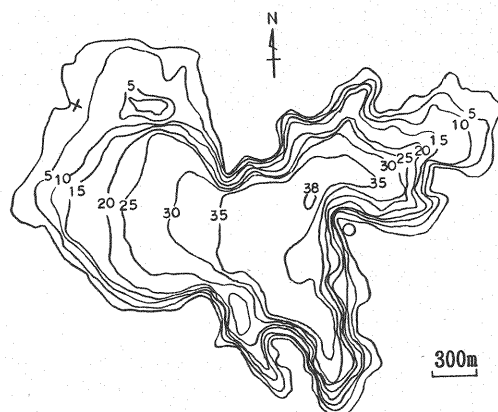


Fig.4 Topography of Lake Nojiri  
(× Pumping Station and Observation station of water level,  
○ that of water temperature)

ride pipe, 20cm in diameter, with a bottom cover and small holes boring through the pipe wall. The observation periods are 2-5 hours. At the beginning and the end of the free water level measurements, vertical profiles of water temperature are measured by scanning a thermistor thermometer from water surface to the bottom with sampling spacings of 1.0m; but in the thermocline region, where the water temperature variance is very large, temperature measurements are made at every 0.5m.

In Lake Nojiri, the typical two-layered state with the thin thermocline region is formed from September to the beginning of October as shown in Fig.12. As the observation of internal seiche, the water temperature in the thermocline region are measured by using a multimodal thermometer with sampling intervals of one minute. As shown in Fig.5, two sensors of thermometer are installed at interval of 1m from the bottom on a wire linking a weight and a buoy which is sinking under water. The sampling periods are two days but the record papers of thermometer are changed after one day.

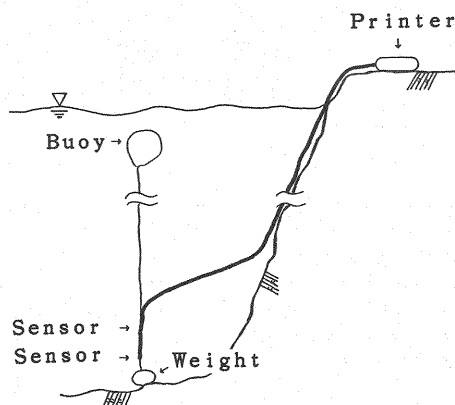


Fig.5 Water temperature observation in thermocline region

#### Lake Suwa

An example of observed time series of the free water level in Lake Suwa is shown in Fig.6. The wind directions observed at Suwa Meteorological Station are WNW during both of the observation periods and the wind velocities range from 3 to 7m/s. Sampling 600 data with interval of 20s and using MEM(Maximum Entropy Method), we computed the power spectra of the free water level variance shown in Fig.7 and the oscillation periods of the variance shown in Table 1. Difference of the mean free water levels between the observations is small and could be neglected in the analysis. Then, the numerical solutions of oscillation period are found to be 1335s, 915s, 797s, 700s, etc. The observation value of the first order is very close to a natural period of longitudinal first mode, 1341s which is

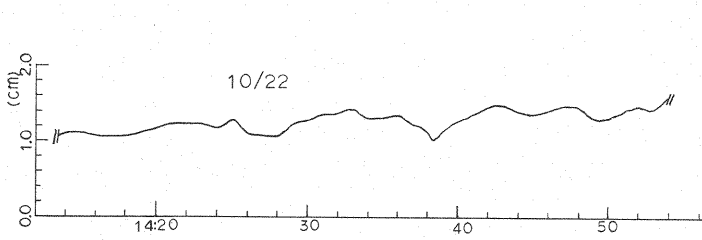


Fig.6 Variance of water level in Lake Suwa

Table 1 Observed oscillation period of free water level (s)

Lake Suwa		
Month /day	first order	second order
10/22	1370	694
11/17	1351	746
Lake Nojiri		
Month /day	first order	second order
8/6	476	345
8/29	470	346
9/26	500	333
9/26	490	333
10/21	479	352
11/25	490	355

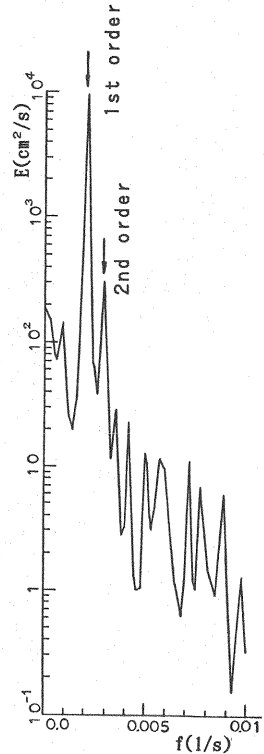


Fig.7 Spectra of free water level variance in Lake Suwa

obtained when Lake Suwa is approximated to be a rectangular lake, 4.0m in depth, 3.0km wide and 4.2km long. So, this period is corresponding to the oscillation period of first mode. And, this period is a little longer than 1250s which was obtained about twenty years ago. The reason of such a difference is due to decrease in water depth in Lake Suwa. During observation, the water temperature is almost kept constant and the maximum amplitude of seiche is less than 1cm, but in other term that is about 5cm at Kamaguchi Water Gate.

#### Lake Nojiri

An example of observed time series of the free water level in Lake Nojiri is shown in Fig.8, and the time-development of temperature profile is also shown in Fig.9. The predominant wind components observed at Tohoku Electric Power Pumping Station are in north and south directions and the wind velocities are less than 4m/s. Sampling 600 data with interval of 10s and using MEM, we obtained the spectra of the free water level variance as shown in Fig.10 and the corresponding oscillation periods of seiche are shown in Table 1. For the one-layered state the numerical solutions of oscillation period are 487s, 362s, 287s, etc.; and the component of 487s is in good agreement with the first order value of Table 1 and also that of 362s is almost near the second order value. Although the observation results are for the one-layered or two-layer states, the difference between them can not be found. This is because the numerical values of natural period of the free surface for the two-layered state are very similar to that for the one-layered state. The maximum amplitudes of seiche in the observation periods and in other term have respectively the same range as those of Lake Suwa.

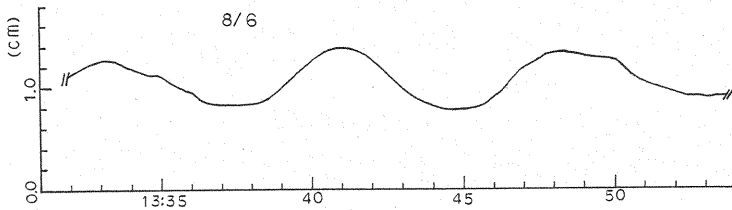


Fig.8 Variance of water level in Lake Nojiri

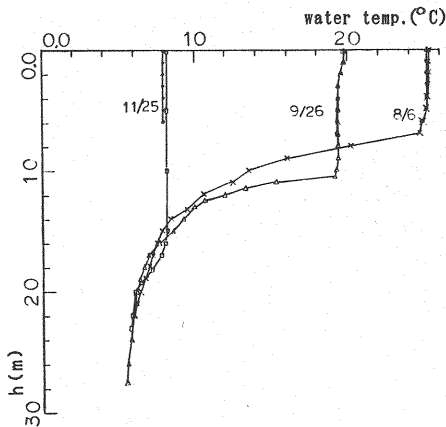


Fig.9 Water temperature profile in Lake Nojiri

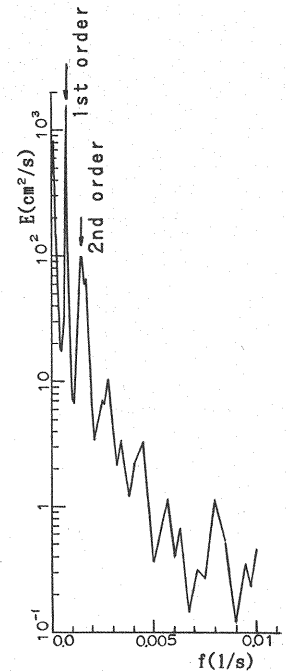


Fig.10 Spectra of free water level variance in Lake Nojiri

To show an example of internal seiche behaviors, the temperature variances observed in the thermocline region are shown in Fig.11,; and the temperature profiles at that time are shown in Fig.12. In addition, an example of spectra of the water temperature variance is shown in Fig.13. In this figure, the numbers of sampling data are 1000-1400 and the sampling period 20s. The observation and numerical values of the temperature oscillation periods are shown in Table 2, where the maximum values of observed oscillation period are shown in the same order position of numerical values, whose value is most near to the maximum ones. Also, because the depth of thermocline was kept almost constant for all observations, the upper layer thickness is fixed to be 10.33m, and the mean water temperatures of upper and lower layers are calculated and the water densities for these temperature are used.

The corresponding numerical and observation values almost coincide with each other, although there exist partially small errors. The reasons of these errors can be considered that there are decision errors of the upper layer thickness and the mean upper and lower layer temperatures, and that the amplitudes of internal seiche are small.

#### CONCLUSION

In this paper, the natural periods of seiche in Lake Suwa and Lake Nojiri were analyzed by using the numerical model and the field observations. A new numerical model for predicting natural periods of seiche in the two-layered lake with the complicated lake shores and lake bottoms were also proposed. The following results are obtained.

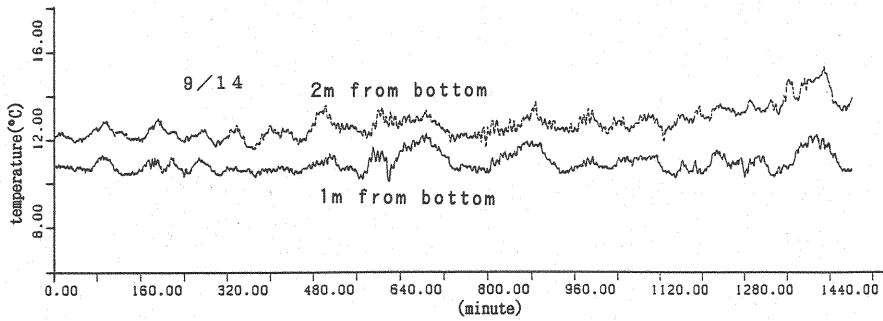


Fig.11 Variance of water temperature in thermocline region of Lake Nojiri

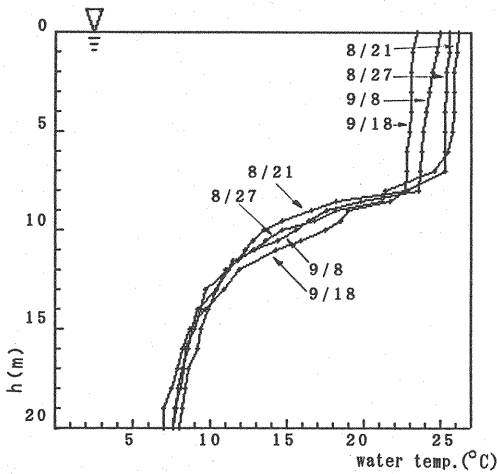


Fig 12 Water temperature profile in Lake Nojiri

Table 2 Oscillation period of water temperature in Lake Nojiri (minute)

Observation value			Numerical value		
Month /day	first order	second order	Month /day	first order	second order
8/26	238		8/26	236	170
8/27		187	8/27	238	171
9/8	250		9/8	245	177
9/9	208		9/9	245	177
9/13		189	9/13	258	186
9/14		172	9/14	258	186
9/16	286		9/16	257	185
9/18	286		9/18	255	184

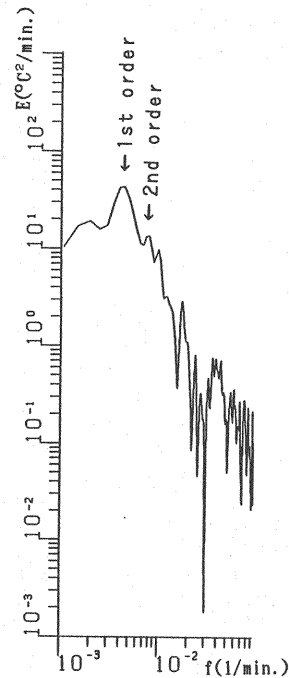


Fig.13 Spectra of water temperature variance in Lake Nojiri

The new model for the natural periods of seiche has been found to be valid by comparing the numerical solutions with the analytical solutions and the observation results. The natural periods of first mode of the surface seiche in Lake



Suwa and Lake Nojiri are about 1350s and 490s, respectively, and also those of the internal seiche in Lake Nojiri vary from 220 to 270 minutes.

#### ACKNOWLEDGMENT

The authors wish to thank N. Yamazaki, a graduate student, for his help in performing observations.

#### REFERENCES

1. Furumoto, K., T. Takemasa, K. Ichinose and Y. Fujikawa : Internal seiche in density stratified lake, Proc. 29th Japanese conference on Hydraulics, pp.389-394, 1985 (in Japanese).
2. Hirata, T. and K. Muraoka : Thermal stratification and internal wave in Lake Chuzenji, Res. Rep. Natl. Inst. Environ. Stud., No.69, pp.5-35, 1984 (in Japanese).
3. Kanari, S. : Internal wave in Lake Biwa (2) ; Numerical experiments with a two layer model , Bulletin of the Disaster Prevention Research Institute, Kyoto University, Vol.22, pp.69-96, 1973.
4. Muraoka, K. and T. Fukushima : Lake current of Kasumigaura(Nishiura), Res. Rep. Natl. Inst. Environ. Stud., No.19, pp.1-150, 1981 (in Japanese).
5. Tayer, C., B.S. Patil and O.C. Zienkiewicz : Harbour oscillation ; A numerical treatment for undamped natural modes, Proc. Inst. Civ. Eng., Vol.43, pp.141-155, 1969.

#### APPENDIX-NOTATION

The following symbols are used in this paper;

$d$	=	depth of internal surface measured from undisturbed free surface;
$\bar{d}$	=	mean depth of internal surface measured from undisturbed free surface;
$d'$	=	depth of internal surface measured from mean internal surface;
$E$	=	spectra of variance
$f$	=	frequency
$g$	=	gravitational acceleration;
$h$	=	depth of water bottom measured from undisturbed free surface;
$N_s$	=	shape function ;
$u_1, v_1$	=	x and y component of mean velocity in upper layer;
$u_2, v_2$	=	x and y component of mean velocity in lower layer;
$T$	=	oscillation period;
$\beta, \gamma$	=	maximum ,or minimum amplitude of harmonic wave;
$\varepsilon$	=	$\rho_1/\rho_2$
$\zeta$	=	water level above undisturbed free surface;
$\lambda^2$	=	$\sigma^2/g$
$\rho_1, \rho_2$	=	densities of upper layer and lower layer and
$\sigma$	=	angular frequency.

(Received October 1, 1991; revised January 23, 1992)